

# Mössbauer spectroscopy of Fe-based nanomaterials

E.P.Yelsukov, G.N.Konygin, V.E.Porsev, E.V.Voronina

Physical-Technical Institute UrB RAS, 132, Kirov St., 426000, Izhevsk, Russia

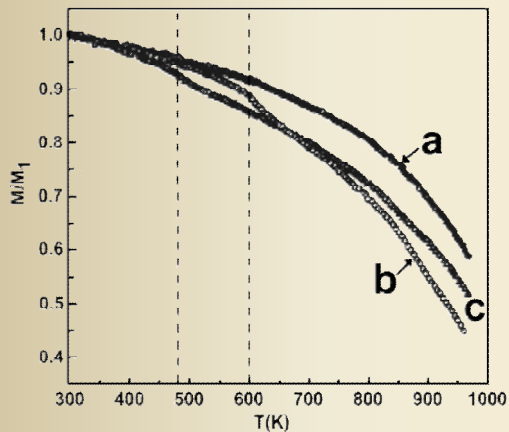
E-mail: [yelsukov@fnms.fti.udm.ru](mailto:yelsukov@fnms.fti.udm.ru)

# 1.Introduction

There are two opinions concerning the effect of the nanosized grains on the magnetic properties and Mössbauer spectra.

1. Nanomaterials ( $\langle L \rangle \leq 10$  nm) have a grain boundary phase (interface region) which has essential differences in the structure, fundamental magnetic properties (saturation magnetization, Curie temperature) and leads to the additional sextet in the Mössbauer spectrum.

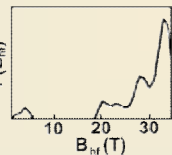
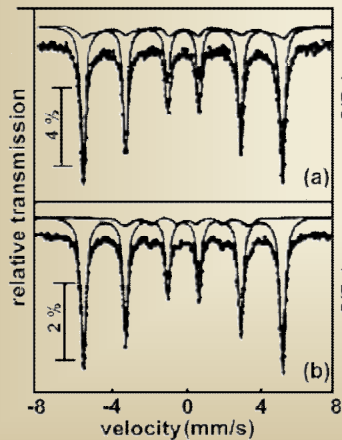
As an example, Del Bianco et al., JMMM, 179-181 (1998) 939



a – un-milled Fe powder

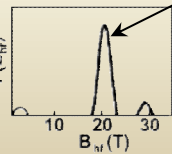
b – as-milled Fe powder ( $\langle L \rangle = 8$  nm)  $t_{\text{mill}} = 32$  h

c – milled powder annealed at 695 K for 14 h



As-milled Fe powder  $t_{\text{mill}} = 32$  h

$\text{Fe}_3\text{C}$  ?

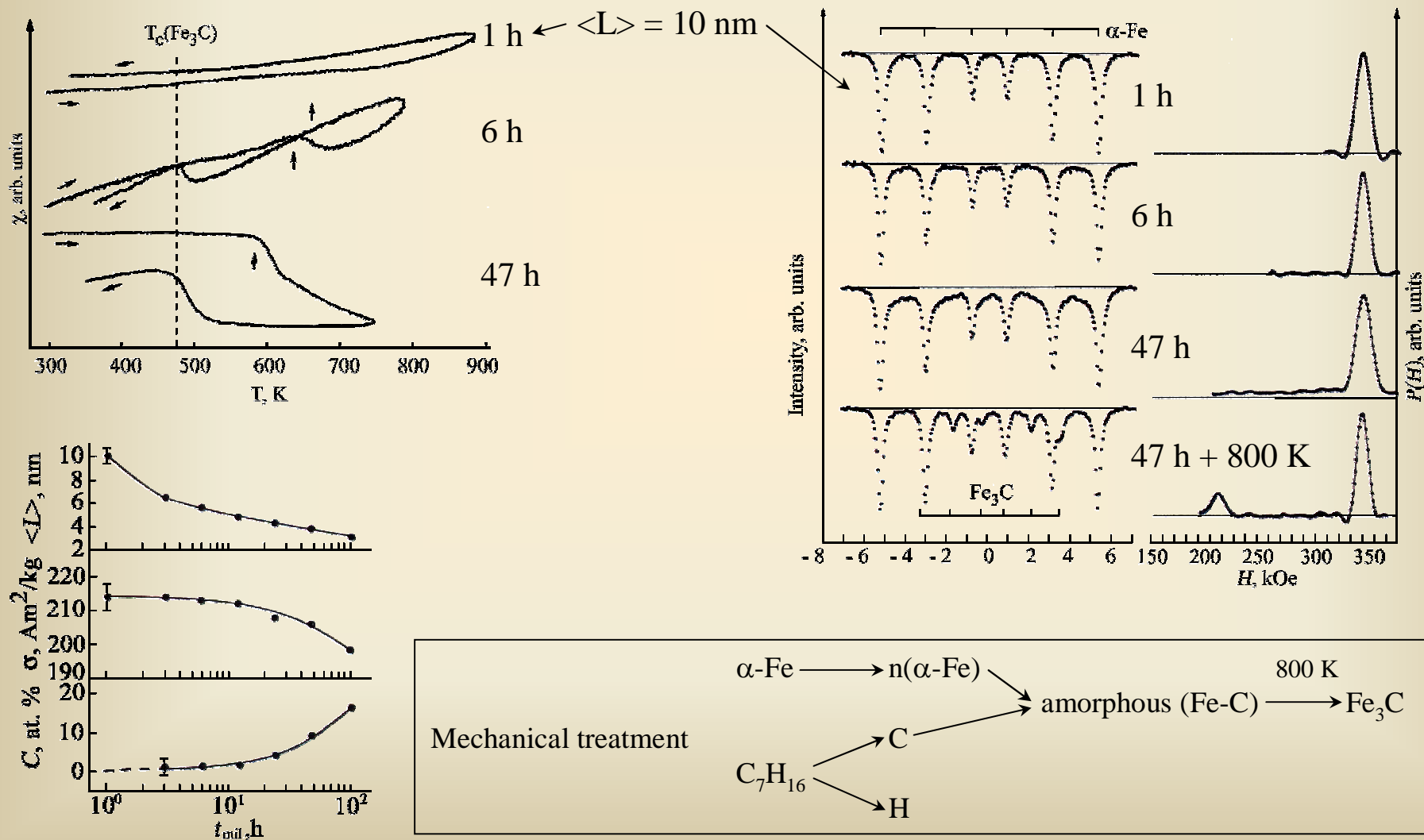


Milled powder annealed at 695 K for 14 h

2. In the absence of the contaminating impurities the nanocrystalline-state formation in  $\alpha$ -Fe does not lead to essential changes in the magnetic properties and Mössbauer spectra.

As an example, Yelsukov et al., Nanostructured Mater., 12 (1999) 483.

Fe milled in a liquid hydrocarbon (heptane  $C_7H_{16}$ ).



The aim of this work was to study how the nanocrystalline state affects the magnetic properties and hyperfine magnetic parameters. The solution of the problem supposes the use of special model objects in which both a nanocrystalline state and a state with the large grain size can be realized, with other conditions being equal.

Along with the  $\alpha$ -Fe, we have chosen Fe-Ge and Fe-Al systems with the broad concentration region (up to 10 at. % Ge and 24 at. Al at 1073 K) of the equilibrium disordered BCC alloys. On the other hand, the BCC disordered nanocrystalline Fe-Ge and Fe-Al alloys can be easily produced by mechanical alloying.

## 2. Experimental

Initial powders with particle size  $\leq 300 \mu\text{m}$

The studied samples:

- $\alpha\text{-Fe}$ 
  - **initial** (un-milled)
  - mechanical grinding for 16 h - **MG (16 h)**
  - annealing of MG (16 h) sample at 773 K for 1 h - **MG (16 h) + 773 K**
- $\alpha\text{-Fe}_{90}\text{Ge}_{10}$ 
  - mechanical alloying for 16 h - **MA (16 h)**
  - after MA (16 h) heating with the rate of 1 K/s up to 1073 K, keeping at 1073 K for 1.5 h, cooling to the room temperature with the rate of 25 K/s - **MA (16 h) + 1073 K**
- $\alpha\text{-Fe}_{77}\text{Al}_{23}$ 
  - mechanical alloying for 16 h - **MA (16 h)**
  - after MA (16 h) heating with the rate of 1 K/s up to 1073 K, keeping at 1073 K for 1.5 h, cooling to the room temperature with the rate of 25 K/s - **MA (16 h) + 1073 K**

**A planetary ball mill Fritsch P-7**

- vials and balls made of hardened steel containing 1 wt. % C and 1.5 wt. % Cr
- power intensity – 2 W/g
- loading – 10 g
- atmosphere – Ar
- heating –  $\leq 60^\circ\text{C}$

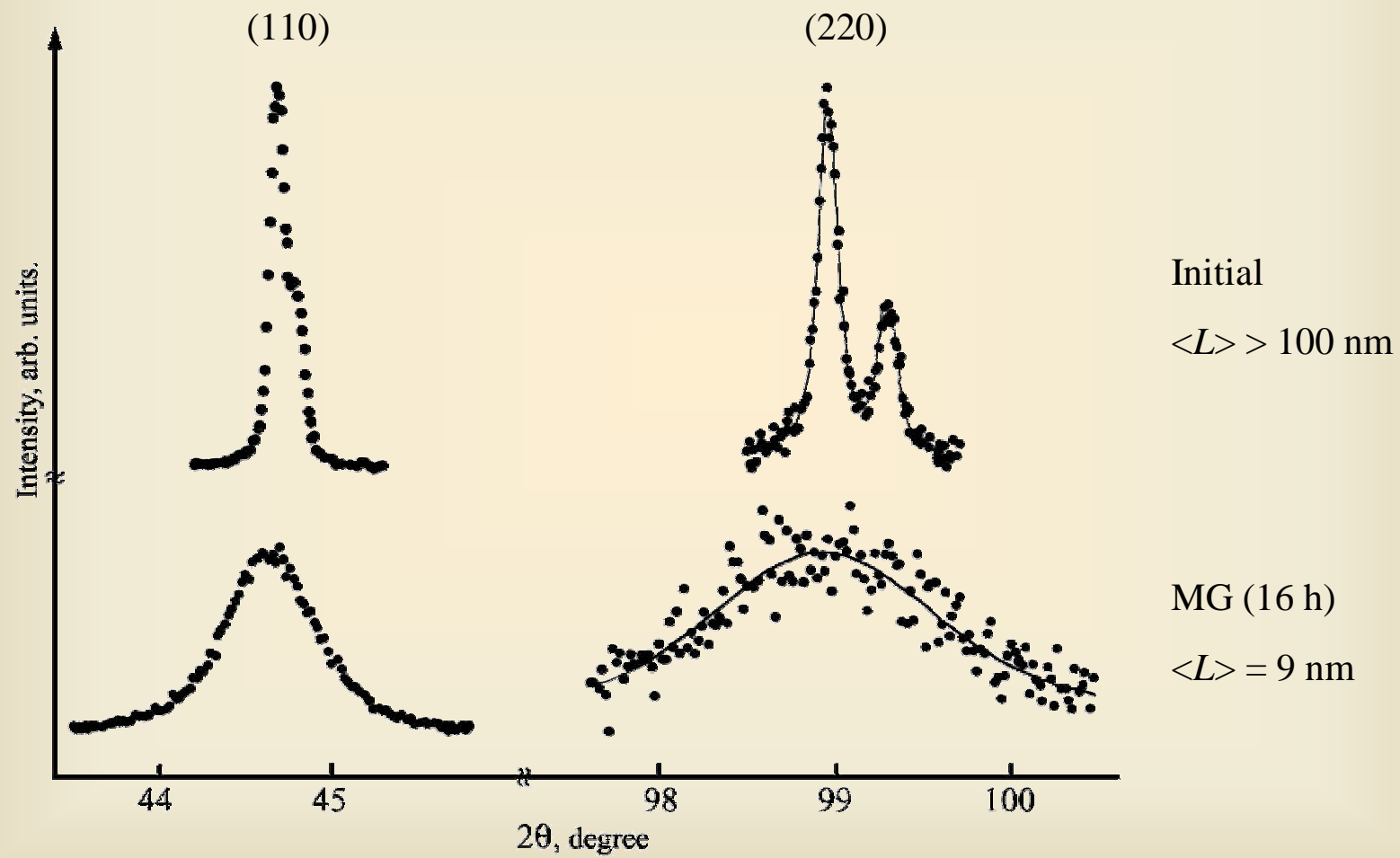
**Experimental techniques**

- post-milling mass increase measurements
- secondary ion mass spectroscopy (SIMS)
- Chemical analysis using Spectraflame – Modula D atomic emission spectrometer
- X-ray diffraction; Mössbauer spectroscopy; Magnetic measurements

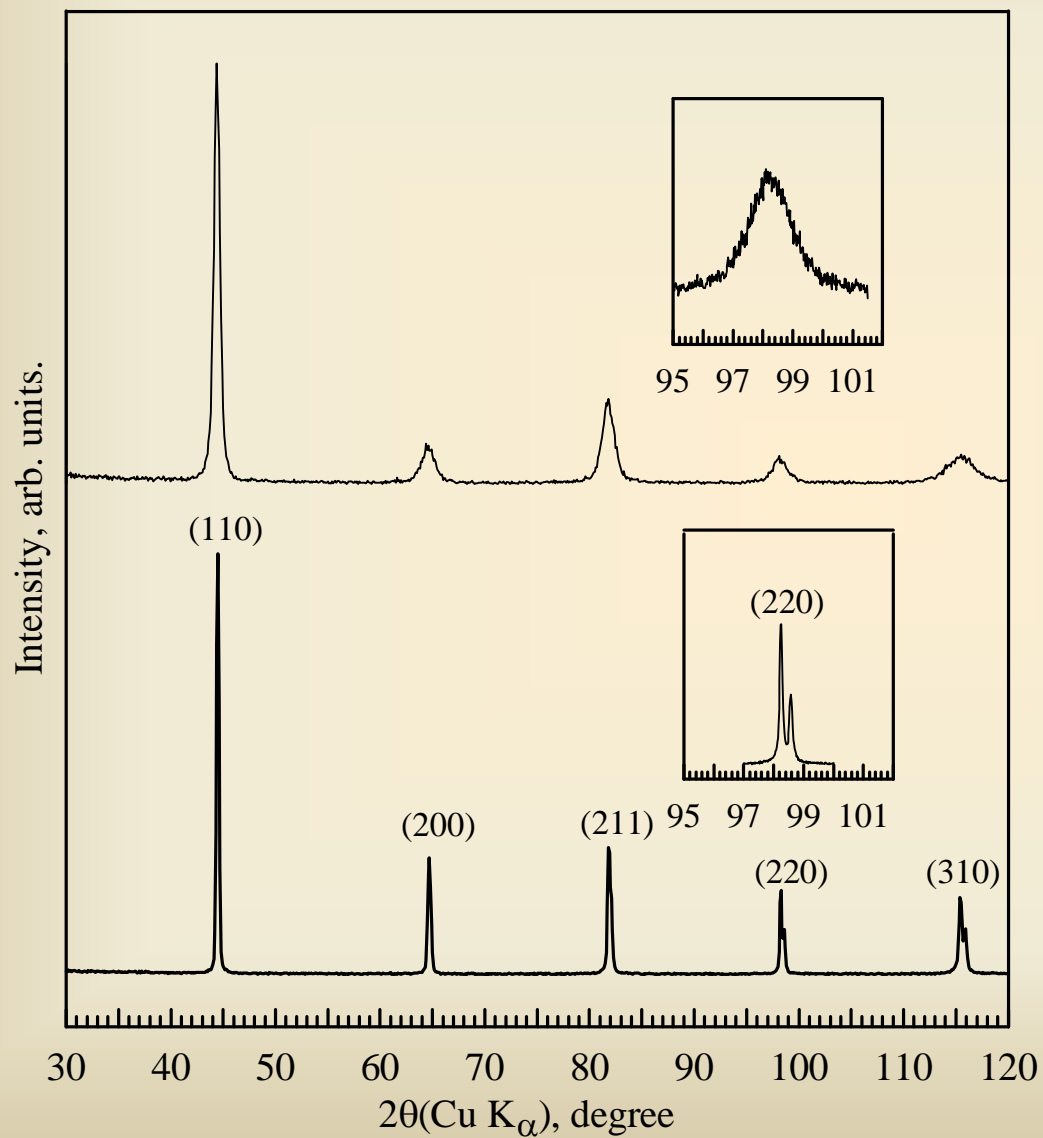
Particles of stone-like shape with average size of 20-40  $\mu\text{m}$ .

The chemical analysis data ( $x_{\text{Ge}} = 9.6$ ,  $x_{\text{Al}} = 22.5$ ,  $x_{\text{Cr}} = 0$ ,  $x_{\text{C}} < 0.3$ ,  $x_{\text{O}} < 0.2$  at. %) as well as the lack of the samples mass change after mechanical treatment demonstrate no detectable amounts Cr, C and O impurities. 5

### 3. X-ray diffraction $\alpha$ -Fe



# $\alpha\text{-Fe}_{90}\text{Ge}_{10}$



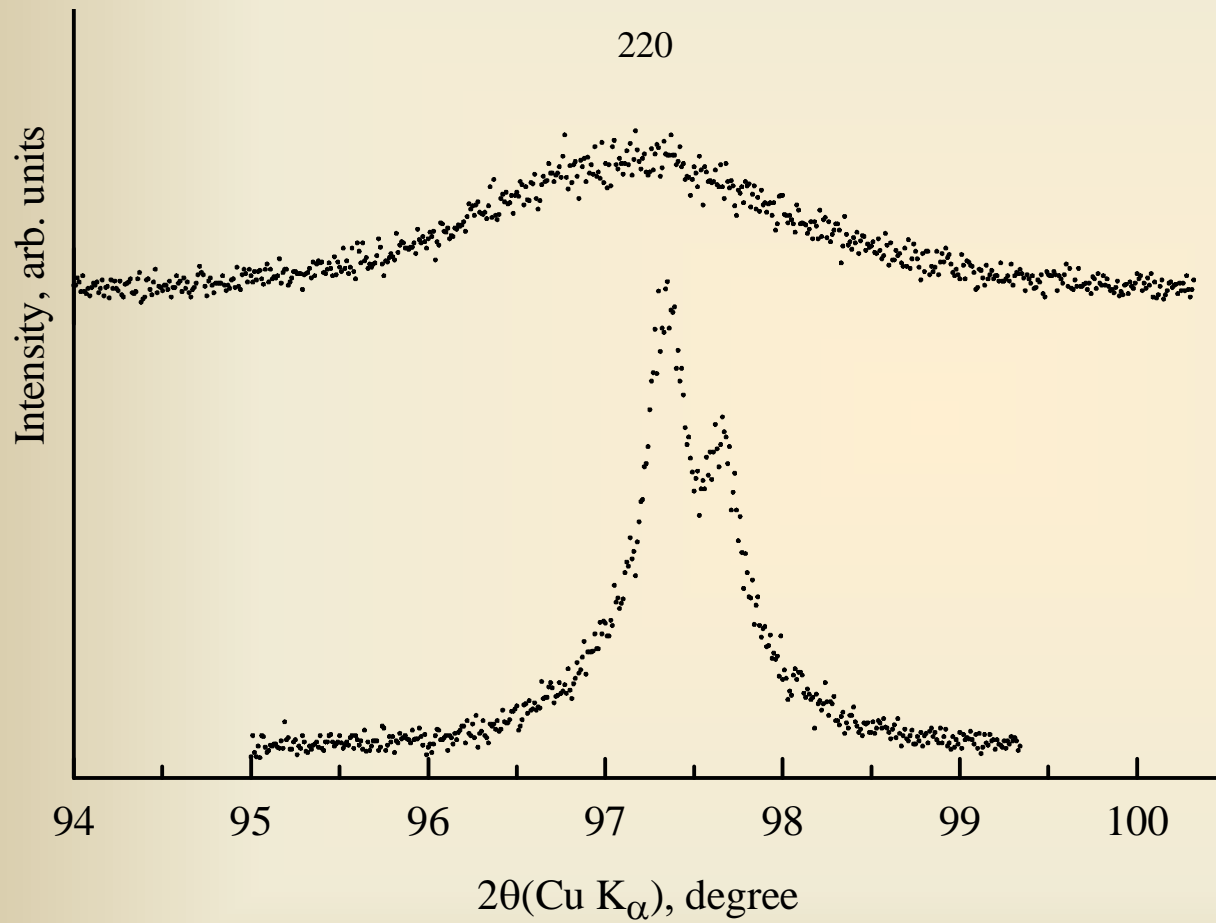
MA (16 h)

$\langle L \rangle = 8 \text{ nm}$

MA (16 h) + 1073 K

$\langle L \rangle > 100 \text{ nm}$

$\alpha\text{-Fe}_{77}\text{Al}_{23}$



MA (16 h)

$\langle L \rangle = 8 \text{ nm}$

MA (16 h) + 1073 K

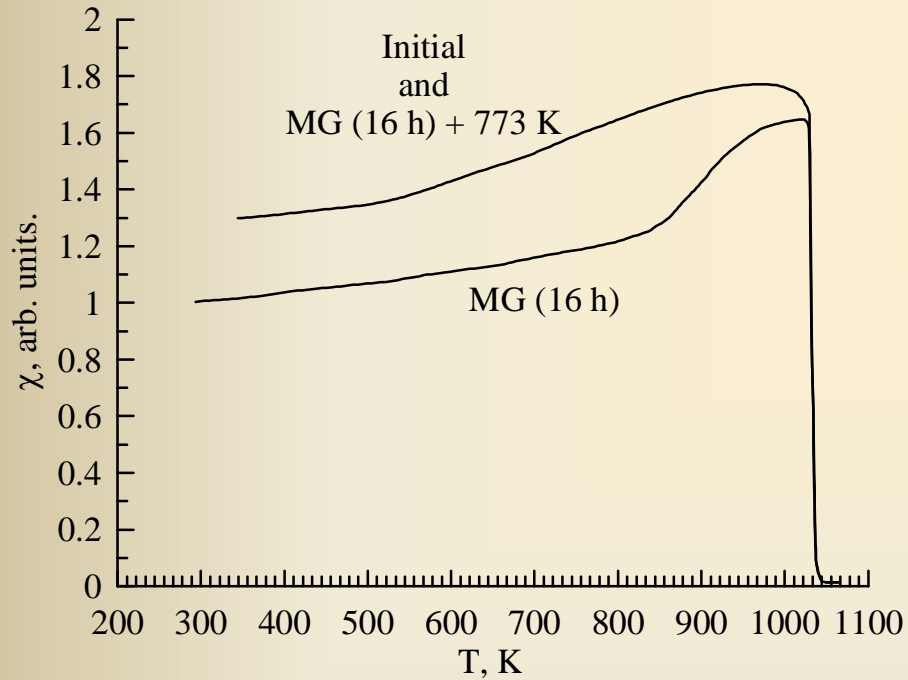
$\langle L \rangle = 30 \text{ nm}$



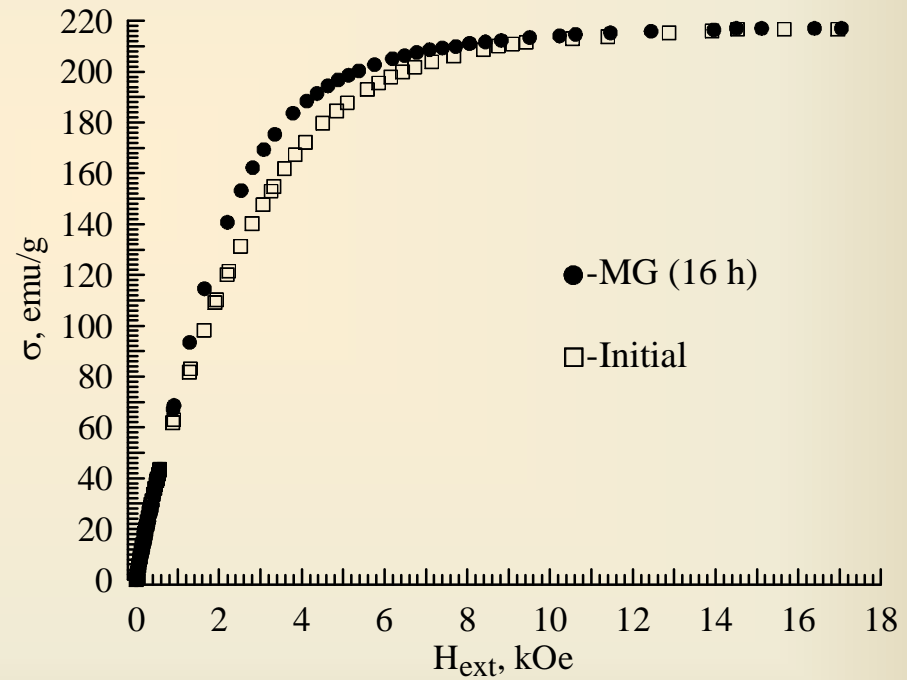
## 4. Magnetic measurements

### $\alpha$ -Fe

Temperature dependences of a.c. magnetic susceptibility (heating rate of 1 K/s)



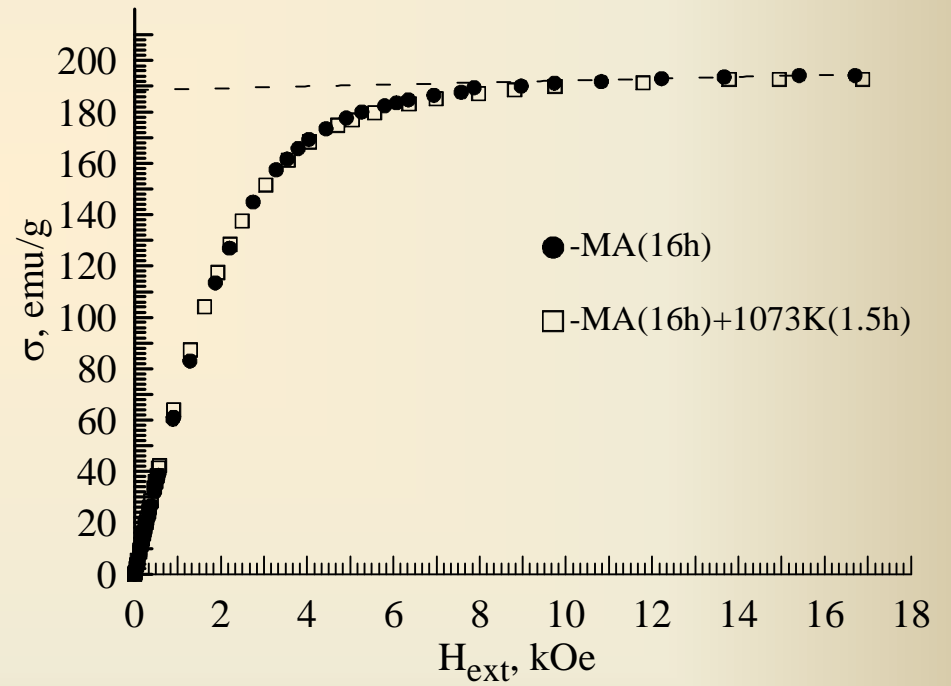
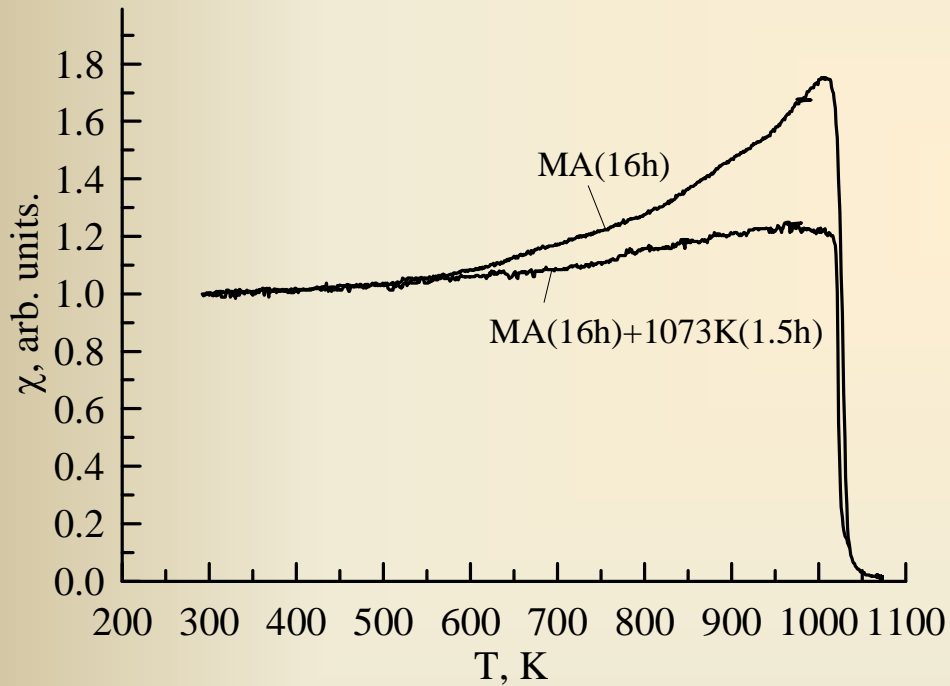
Magnetization curves ( $T_{\text{meas}} = 300$  K)



# $\alpha\text{-Fe}_{90}\text{Ge}_{10}$

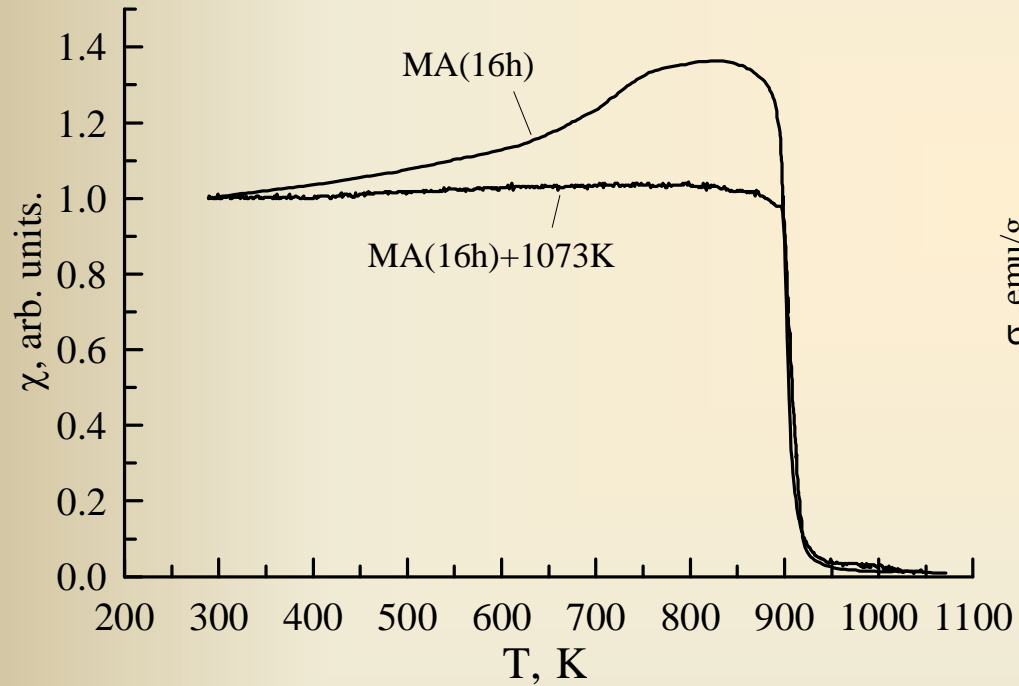
Temperature dependences of a.c. magnetic susceptibility (heating rate of 1 K/s)

Magnetization curves ( $T_{\text{meas}} = 300$  K)

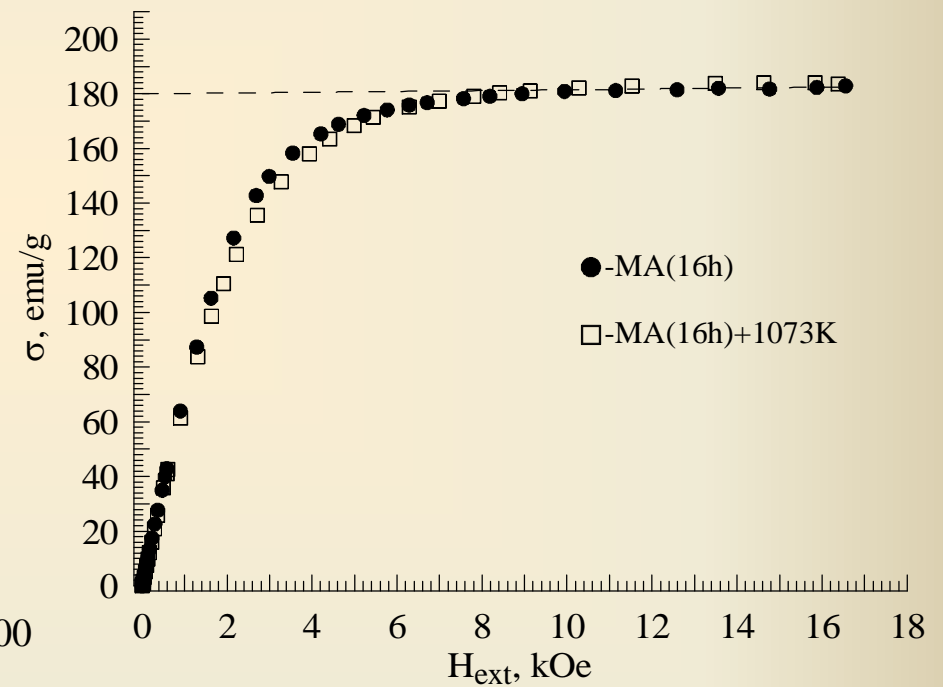


# $\alpha\text{-Fe}_{77}\text{Al}_{23}$

Temperature dependences of a.c. magnetic susceptibility (heating rate of 1 K/s)



Magnetization curves ( $T_{\text{meas}} = 77 \text{ K}$ )



# $\alpha\text{-Fe}_{77}\text{Al}_{23}$

ZFC and FC curves

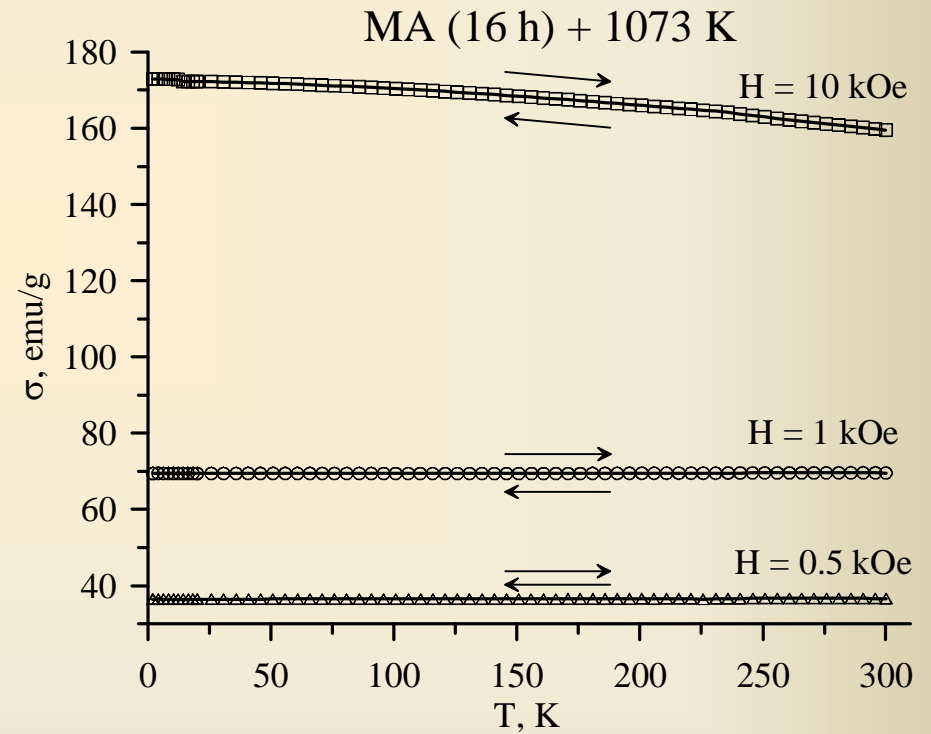
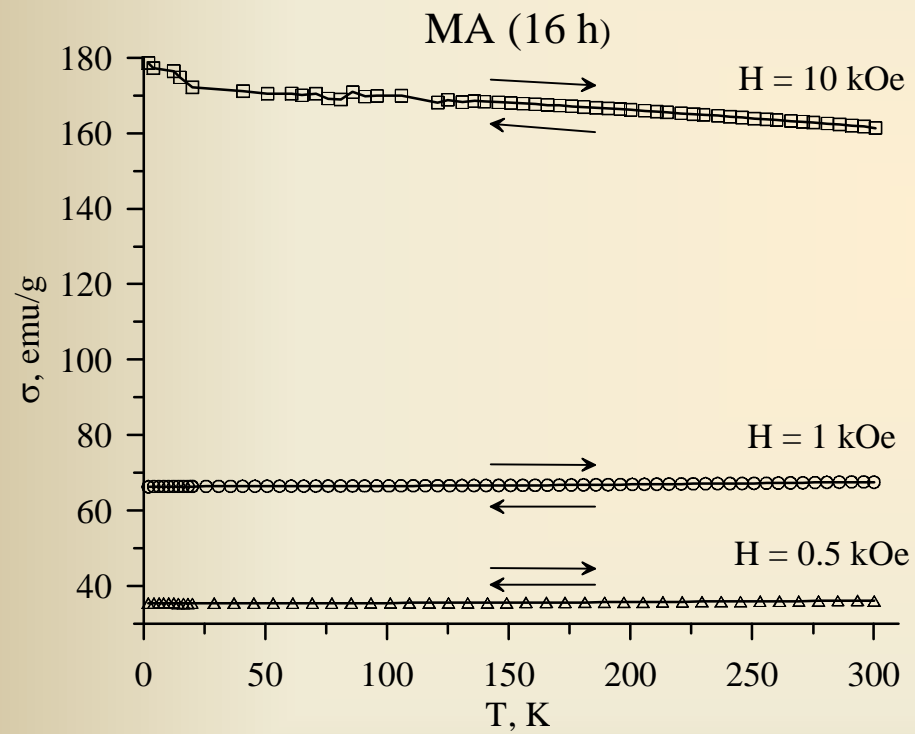


Table 1. Structural and magnetic parameters of the nanocrystalline and annealed alloys.

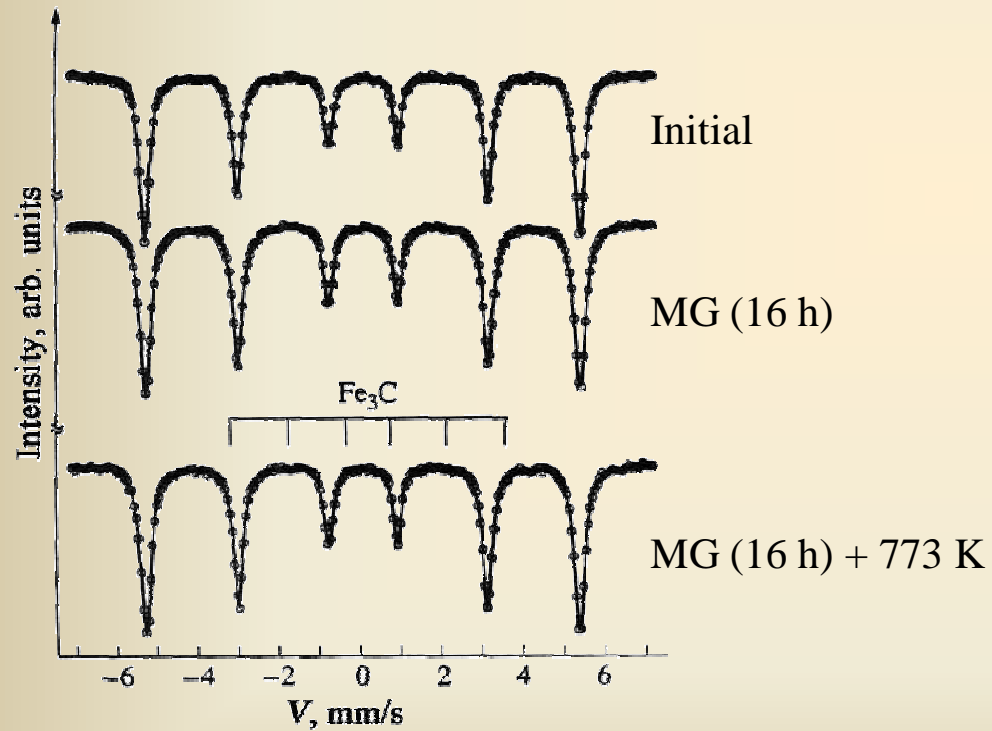
Sample		$a$ , nm	$\langle L \rangle$ , nm	$\langle \varepsilon^2 \rangle^{1/2}$ , %	$\sigma_0$ , emu/g	$T_c$ , K
$\alpha$ -Fe	MG (16 h)	$0.2869_1^*$	$9_1$	$0.22_2$	$217_2$ (300 K)	$1040_8$
	Initial	$0.2866_1$	$> 100$	$0.03_1$	$217_2$ (300 K)	$1043_3$
$\alpha$ -Fe <sub>90</sub> Ge <sub>10</sub>	MA (16 h)	$0.2884_1$	$8_1$	$0.26_2$	$188_2$ (300 K)	$1017_3$
	MA(16 h) + 1073 K	$0.2881_1$	$> 100$	$0.01_1$	$188_2$ (300 K)	$1020_3$
$\alpha$ -Fe <sub>77</sub> Al <sub>23</sub>	MA (16 h)	$0.2907_1$	$8_1$	$0.32_3$	$180_2$ (77 K)	$890_3$
	MA(16 h) + 1073 K	$0.2903_1$	$30_3$	$0.04_1$	$180_2$ (77 K)	$895_3$

\* The subscript denotes uncertainty in the last digit of the tabulated value.

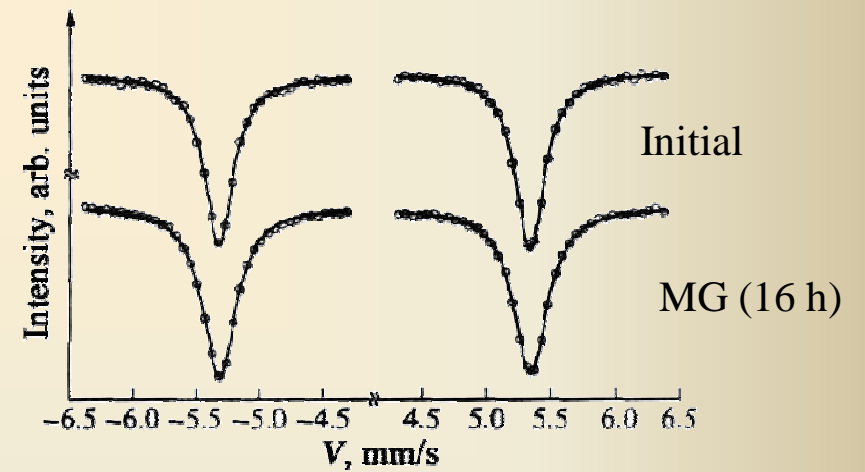
- Transition into a nanocrystalline state results in a small increase of the bcc lattice parameter and a microstrain growth;
- The  $\sigma_0$  and  $T_c$  values remain unchanged;
- No features are found in the  $\chi$  (T) dependences of the nanostructured samples.

## 5. Mössbauer spectroscopy $\alpha$ -Fe

Mössbauer spectra of different samples of iron powder

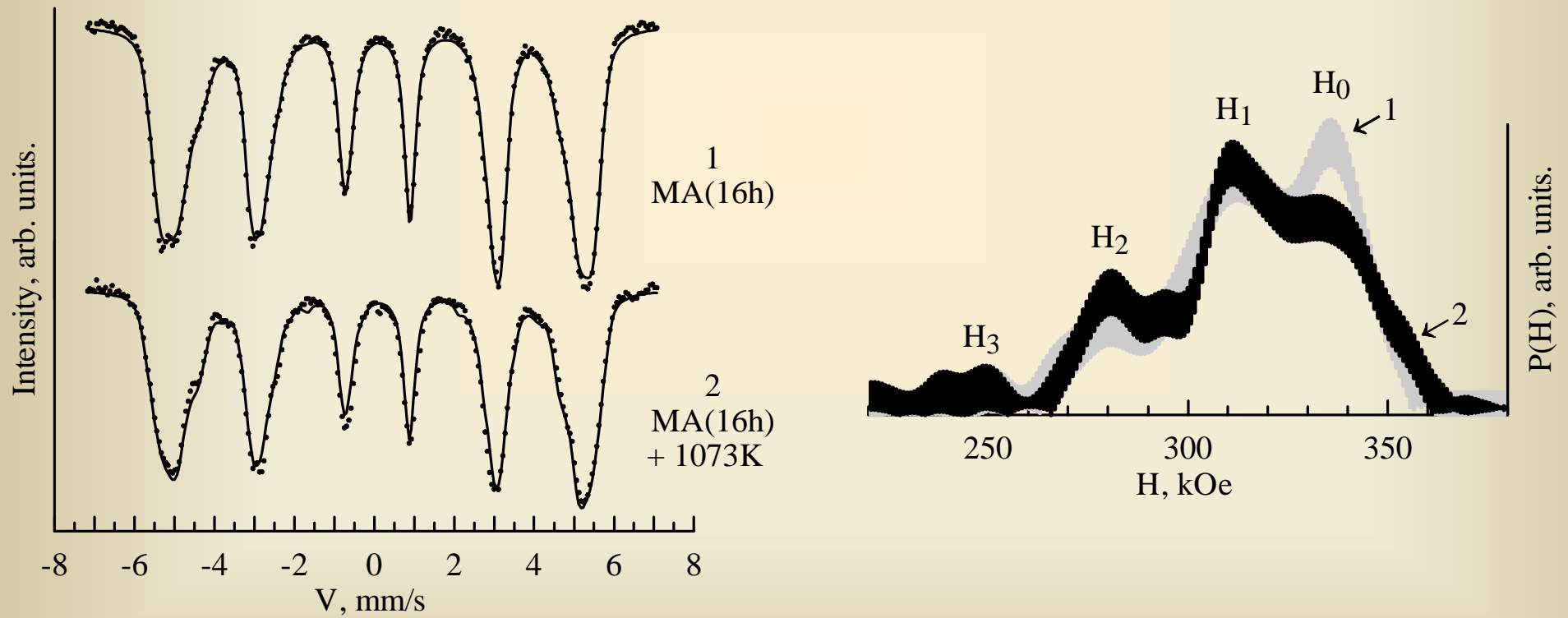


Parts of the Mössbauer spectra showing the 1<sup>st</sup> and 6<sup>th</sup> peaks



# $\alpha\text{-Fe}_{90}\text{Ge}_{10}$

Mössbauer spectra and corresponding distributions  $P(H)$  of mechanically alloyed and annealed samples



# $\alpha\text{-Fe}_{77}\text{Al}_{23}$

Mössbauer spectra and corresponding distributions  $P(H)$  of mechanically alloyed and annealed samples

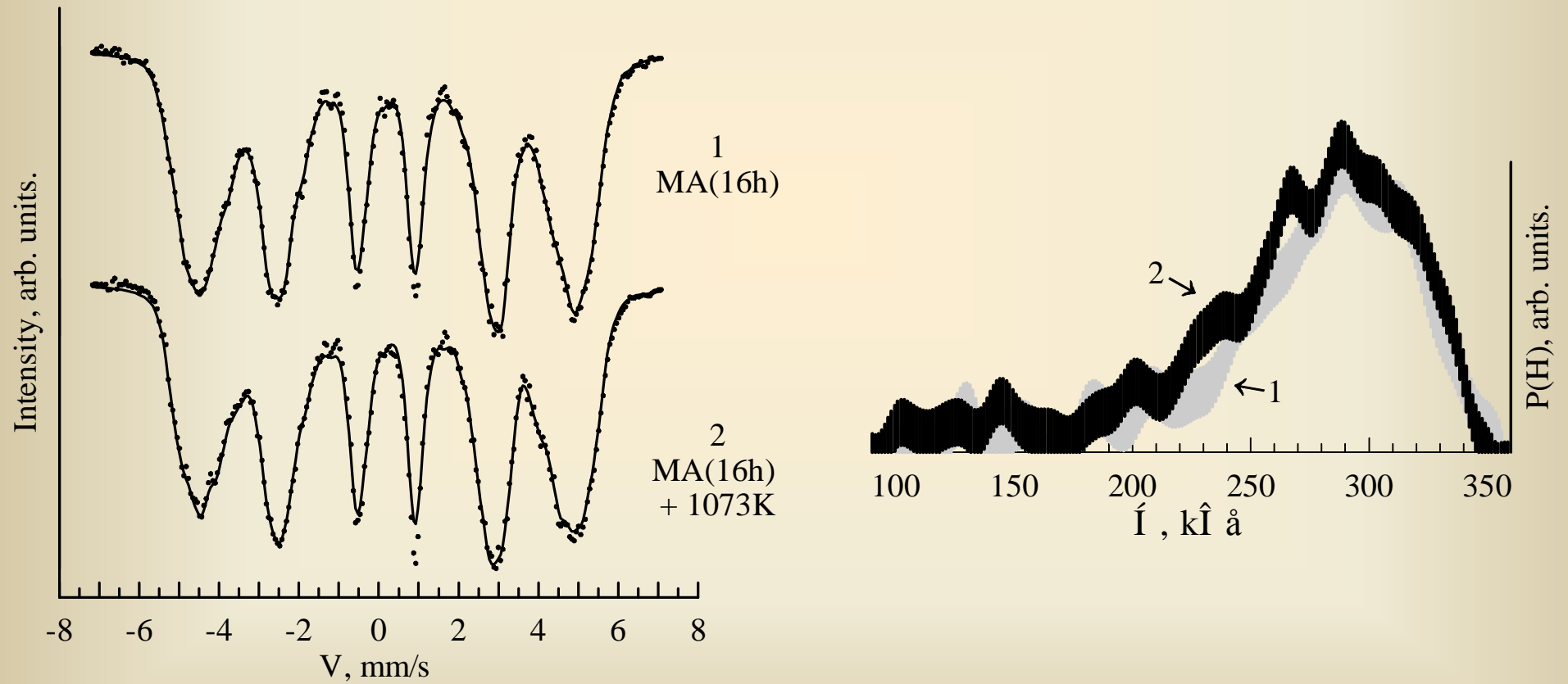




Table 2. Average hyperfine parameters of the nanocrystalline and annealed alloys.

Sample		$\Gamma_{1,6}$ , mm/s	$\bar{\delta}$ , mm/s	$\bar{H}$ , kOe
$\alpha$ -Fe	MG (16 h)	$0.32_1$	$0.01_1^*$	$331.1_5$ (300 K)
	Initial	$0.27_1$	$0.01_1$	$331.0_5$ (300 K)
$\alpha$ -Fe <sub>90</sub> Ge <sub>10</sub>	MA (16 h)	$1.01_3$	$0.09_2$	$314_2$ (300 K)
	MA(16 h) + 1073 K	$1.14_3$	$0.09_2$	$313_3$ (300 K)
$\alpha$ -Fe <sub>77</sub> Al <sub>23</sub>	MA (16 h)	$1.47_3$	$0.20_3$	$275_3$ (77 K)
	MA(16 h) + 1073 K	$1.56_3$	$0.20_3$	$267_3$ (77 K)

\* Relative to  $\alpha$ -Fe at room temperature.

- There is no new component in MS of the nanocrystalline  $\alpha$ -Fe, the MS lines width increases by 20%;
- The  $\bar{\delta}$  and  $\bar{H}$  parameters remain unchanged for all samples;
- The lines width of the annealed Fe<sub>90</sub>Ge<sub>10</sub> and Fe<sub>77</sub>Al<sub>23</sub> samples is more than that of the mechanically alloyed ones.

Table 3. Fractions of area ( $P_k$ ) of the Mössbauer spectrum and local atomic configurations probabilities calculated for bcc disordered alloy  $\text{Fe}_{90}\text{Ge}_{10}$ .

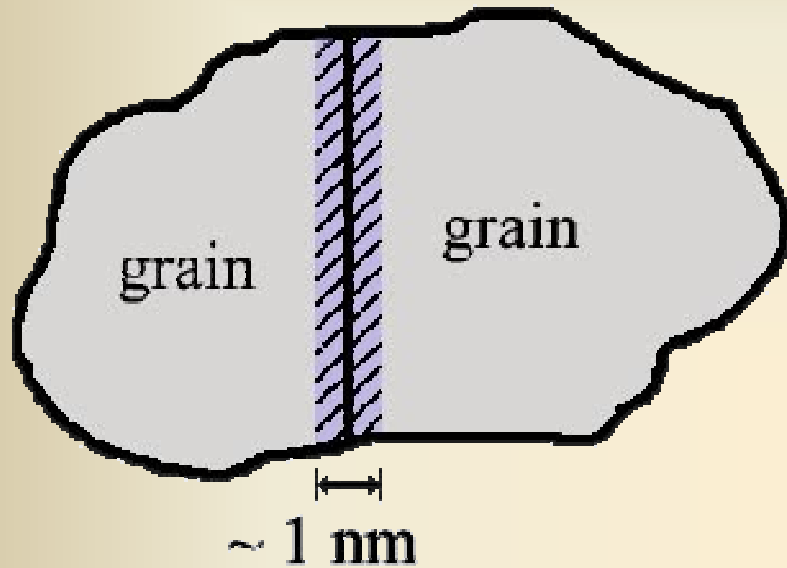
Sample	$P_0, \%$	$P_1, \%$	$P_2, \%$	$P_3, \%$	$P_4, \%$
MA(16h)	$43.3 \pm 1$	$38.8 \pm 1$	$15.7 \pm 1$	$2.2 \pm 2$	—
MA(16h) + 1073K	$35.2 \pm 1$	$43.0 \pm 1$	$19.9 \pm 1$	$1.9 \pm 2$	—
Calculated using Binominal Distribution	43.05	38.26	14.88	3.31	0.05

Table 4. Local hyperfine magnetic fields and isomer shifts of mechanically alloyed – MA(16h) and with following annealing – MA(16h) + 1073K Fe<sub>90</sub>Ge<sub>10</sub>.

	MA(16h)	MA(16h) + 1073K
H <sub>0</sub> , kOe	336 ± 2	338 ± 2
H <sub>1</sub> , kOe	311 ± 2	314 ± 2
H <sub>2</sub> , kOe	281 ± 3	284 ± 3
H <sub>3</sub> , kOe	252 ± 5	244 ± 5
I <sub>0</sub> <sup>*</sup> , mm/s	0.05 ± 0.02	0.05 ± 0.02
I <sub>1</sub> , mm/s	0.10 ± 0.02	0.09 ± 0.02
I <sub>2</sub> , mm/s	0.15 ± 0.02	0.15 ± 0.02
I <sub>3</sub> , mm/s	0.20 ± 0.04	0.25 ± 0.04

\* Relative to α-Fe at room temperature.

## $\alpha$ -Fe



Interface region

(boundary and close-to-boundary distorted zones)

Initial ( $\langle L \rangle > 100$  nm)  $\rightarrow \Gamma_{1,6} = 0.27$  mm/s

MG (16 h) ( $\langle L \rangle = 8$  nm)  $\rightarrow \Gamma_{1,6} = 0.32$  mm/s

The increase of  $\Gamma$  can be accounted for by a different in values and sign anisotropic contribution to HFMF for Fe atoms in interface regions.

$$H = H_{is} + H_{anis}$$

$$H_{anis} = \frac{1}{2} h(3\cos^2\theta - 1)$$

Grain:  $\theta = 54^\circ 30'$   $\rightarrow H_{anis} = 0$

Interface region: distribution of  $\theta \rightarrow$

distribution of  $H_{anis} \rightarrow$

$\Gamma(\text{MG}) > \Gamma(\text{Initial})$

## 6. Conclusions

1. With the absence of contamination no changes have been found in the specific saturation magnetization, Curie temperature and hyperfine interaction parameters;
2. No additional sextets in the Mössbauer spectra and features in the temperature dependences of a.c. magnetic susceptibility were found either;
3. A slight broadening ( $\sim 20\%$ ) in the Mössbauer spectrum of the nanocrystalline pure Fe is explained by random in sign and magnitude anisotropic contribution to the HFMF from the Fe atoms in interface region of nanostructure.

### Acknowledgements

The authors would like to express their gratitude to Drs. A.V.Korolyov, A.V.Zagainov, N.B.Arsentyeva and O.M.Nemtsova for the support of the experiment of this work.

**Thank you very much for your attention!**